Enhancement of HIV-1 infectivity by simple, self-assembling modular peptides

David Easterhoff[1,#], John T. M. DiMaio[2,#], Todd M. Doran[2], Stephen Dewhurst[1,*], Bradley L. Nilsson[2,*]

From the Departments of [1]Microbiology and Immunology, and [2]Chemistry, University of Rochester, Rochester, NY 14627

SUPPORTING MATERIAL

Contents:

Figure S1. CD spectral analysis of cationic peptides in phosphate-buffered saline (PBS)	**S2**
Figure S2. CD spectral analysis of anionic peptides in PBS	**S3**
Figure S3. Analytical HPLC trace (215 nm) of peptide Ac-$K_2(AKAE)_2$-NH_2	**S4**
Figure S4. Analytical HPLC trace (215 nm) of peptide Ac-$K_2(FKFE)_2$-NH_2	**S4**
Figure S5. Analytical HPLC trace (215 nm) of peptide Ac-$K_4(FKFE)_2$-NH_2	**S4**
Figure S6. Analytical HPLC trace (215 nm) of peptide Ac-$K_2(ChaKChaE)_2$-NH_2	**S5**
Figure S7. Analytical HPLC trace (215 nm) of peptide Ac-$K_4(ChaKChaE)_2$-NH_2	**S5**
Figure S8. Analytical HPLC trace (215 nm) of peptide Ac-$E_2(FKFE)_2$-NH_2	**S5**
Figure S9. Analytical HPLC trace (215 nm) of peptide Ac-$E_4(FKFE)_2$-NH_2	**S6**
Figure S10. Analytical HPLC trace (215 nm) of peptide Ac-$E_2(ChaKChaE)_2$-NH_2	**S6**
Figure S11. Analytical HPLC trace (215 nm) of peptide Ac-$E_4(ChaKChaE)_2$-NH_2	**S6**
Table S1. Analytical HPLC conditions of peptides **1-9**	**S7**
Figure S12. MALDI mass spectrum of Ac-$K_2(AKAE)_2$-NH_2	**S8**
Figure S13. MALDI mass spectrum of Ac-$K_2(FKFE)_2$-NH_2	**S8**
Figure S14. MALDI mass spectrum of Ac-$K_4(FKFE)_2$-NH_2	**S9**
Figure S15. MALDI mass spectrum of Ac-$K_2(ChaKChaE)_2$-NH_2	**S9**
Figure S16. MALDI mass spectrum of Ac-$K_4(ChaKChaE)_2$-NH_2	**S10**
Figure S17. MALDI mass spectrum of Ac-$E_2(FKFE)_2$-NH_2	**S10**
Figure S18. MALDI mass spectrum of Ac-$E_4(FKFE)_2$-NH_2	**S11**
Figure S19. MALDI mass spectrum of Ac-$E_2(ChaKChaE)_2$-NH_2	**S11**
Figure S20. MALDI mass spectrum of Ac-$E_4(ChaKChaE)_2$-NH_2	**S12**
Figure S21. Visible appearance of peptide supramolecular assemblies.	**S13**
Figure S22. TEM images of peptide supramolecular assemblies, before and after removal of insoluble material by centrifugal sedimentation.	**S14**
Figure S23. Cationic peptide supramolecular assemblies efficiently enhance low dose HIV-1 infection.	**S16**
Figure S24. Cationic and anionic supramolecular assemblies are not cytotoxic	**S17**

Figure S1. (**A**-**E**) The cationic peptides were examined via CD in phosphate buffered saline in parallel to the experiments performed in unbuffered water. **A**-**D** all exhibit characteristics of β-sheet assemblies without the addition of NaCl (other than that already present in the buffer). **E** exhibited characteristics of a unordered structure orientation. All peptides were at 300 μM. (**A**) Ac-$K_2(FKFE)_2$-NH_2. (**B**) Ac-$K_4(FKFE)_2$-NH_2. (**C**) Ac-$K_2(ChaKChaE)_2$-NH_2. (**D**) Ac-$K_4(ChaKChaE)_2$-NH_2. (E) Ac-$K_2(AKAE)_2$-NH_2.

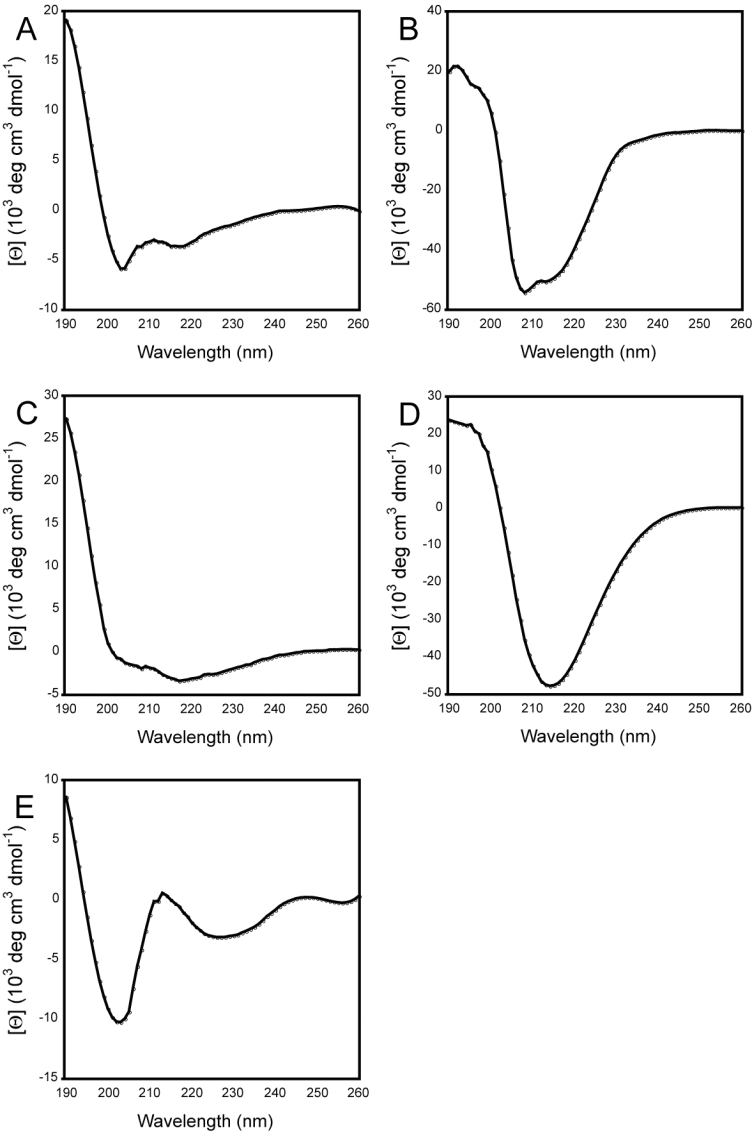

Figure S2. (**A**-**D**) The anionic peptides were examined via CD in phosphate buffered saline to parallel the experiments performed in unbuffered water. **A**, **C**, and **D** all exhibited characteristics of β-sheet assemblies without the addition of NaCl (other than that already present in the buffer). **B** initially showed evidence of an unordered structure, however, after addition of NaCl there was evidence of β-sheet assembly, which is consistent with the previous experiments. All peptides were at 300 μM. (**A**) Ac-$E_2(FKFE)_2$-NH_2. (**B**) Ac-$E_4(FKFE)_2$-NH_2. (**C**) Ac-$E_2(ChaKChaE)_2$-NH_2. (**D**) Ac-$E_4(ChaKChaE)_2$-NH_2.

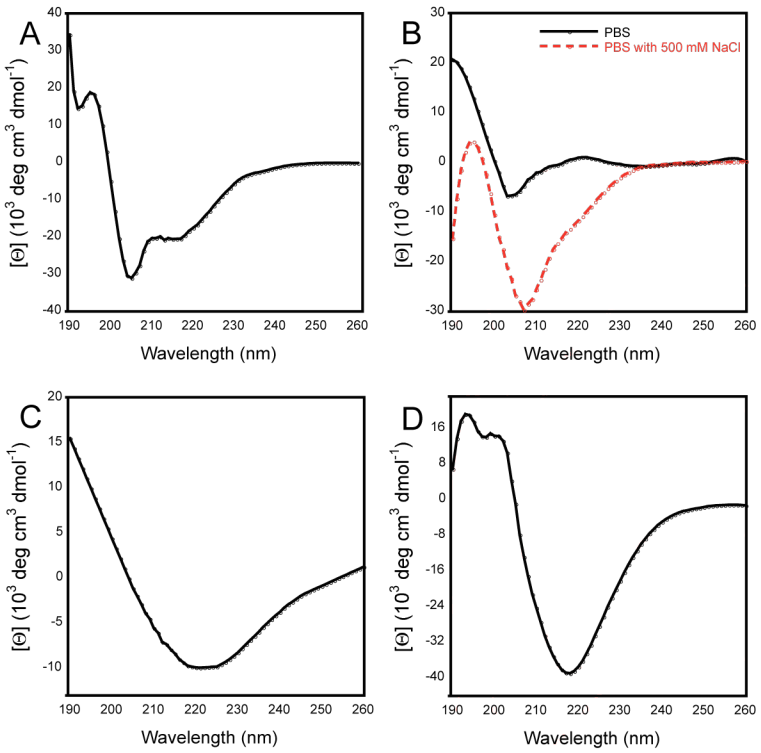

Figure S3. Analytical HPLC trace (215 nm) of Ac-$K_2(AKAE)_2$-NH_2.

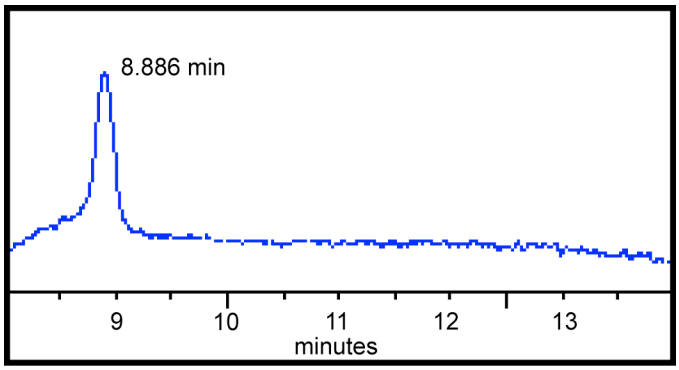

Figure S4. Analytical HPLC trace (215 nm) of Ac-$K_2(FKFE)_2$-NH_2.

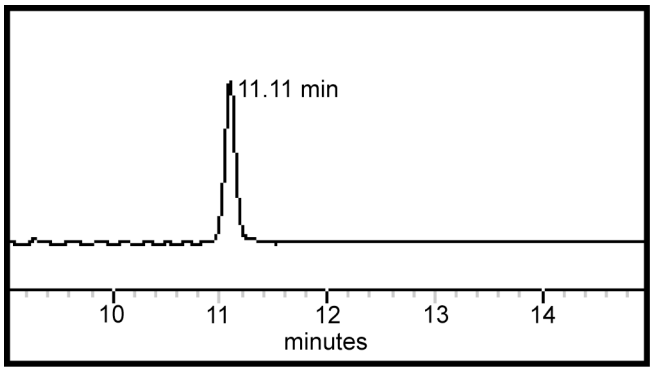

Figure S5. Analytical HPLC trace (215 nm) of Ac-$K_4(FKFE)_2$-NH_2.

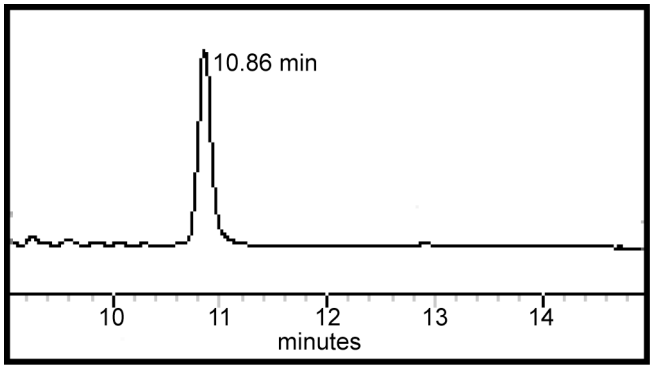

Figure S6. Analytical HPLC trace (215 nm) of Ac-K_2(ChaKChaE)$_2$-NH_2.

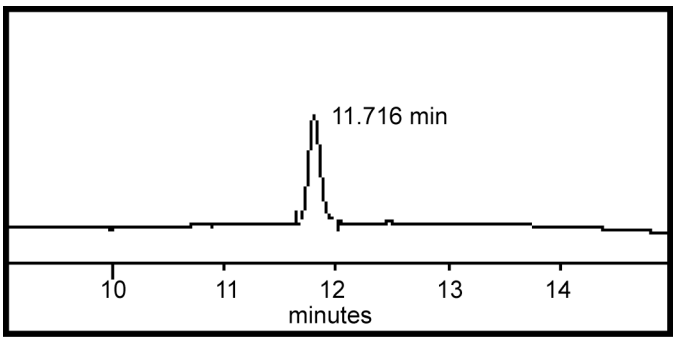

Figure S7. Analytical HPLC trace (215 nm) of Ac-K_4(ChaKChaE)$_2$-NH_2.

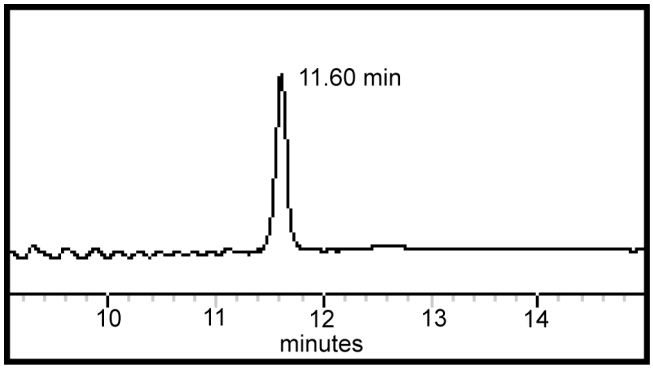

Figure S8. Analytical HPLC trace (215 nm) of Ac-E_2(FKFE)$_2$-NH_2.

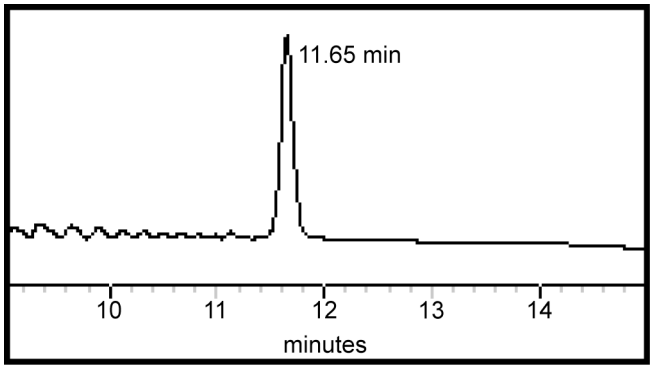

Figure S9. Analytical HPLC trace (215 nm) of Ac-$E_4(FKFE)_2$-NH_2.

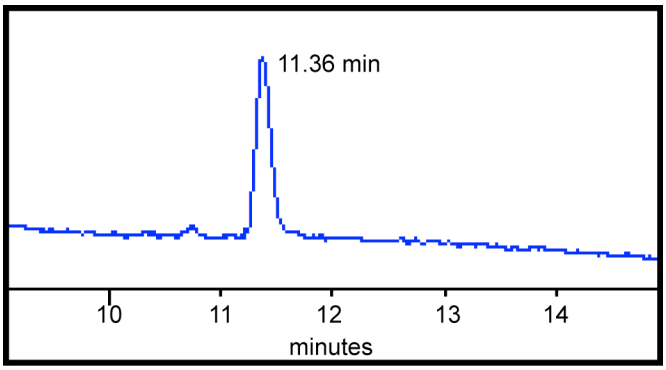

Figure S10. Analytical HPLC trace (215 nm) of Ac-$E_2(ChaKChaE)_2$-NH_2.

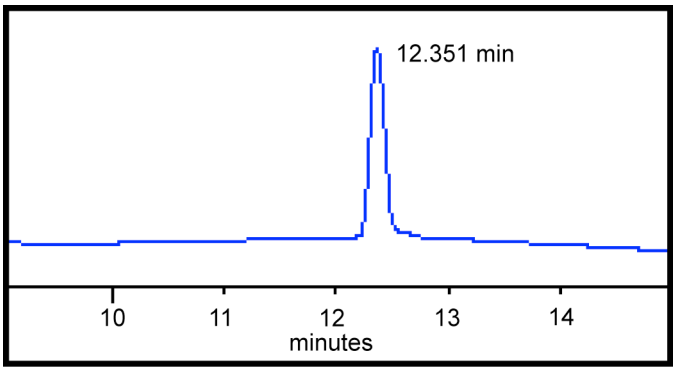

Figure S11. Analytical HPLC trace (215 nm) of Ac-$E_4(ChaKChaE)_2$-NH_2.

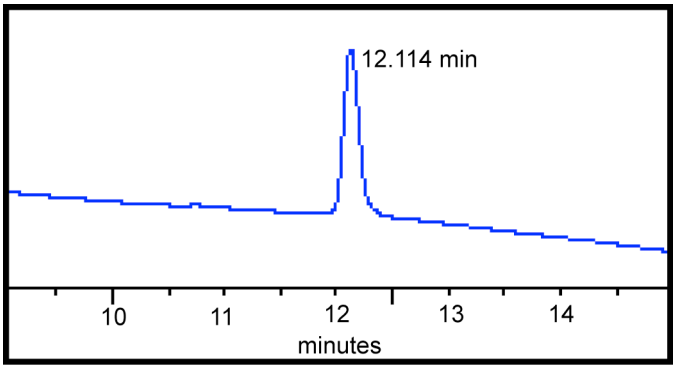

Table S1. Analytical HPLC conditions for peptides **1-9.**

Peptide	**Sequence**	**Retention Time** (min)	**Gradient** (soln A: water/0.5% TFA; soln B: acetonitrile/0.5% TFA
1	Ac-K_2(FKFE)$_2$-NH_2	11.11	Isocratic 5% **B** 5 min, 5-95% **B** over 10 min, 95% **B** 5 min
2	Ac-K_4(FKFE)$_2$-NH_2	10.86	Isocratic 5% **B** 5 min, 5-95% **B** over 10 min, 95% **B** 5 min
3	Ac-K_2(ChaKChaE)$_2$-NH_2	11.716	Isocratic 5% **B** 5 min, 5-95% **B** over 10 min, 95% **B** 5 min
4	Ac-K_4(ChaKChaE)$_2$-NH_2	11.60	Isocratic 5% **B** 5 min, 5-95% **B** over 10 min, 95% **B** 5 min
5	Ac-K_2(AKAE)$_2$-NH_2	8.886	Isocratic 5% **B** 5 min, 5-95% **B** over 10 min, 95% **B** 5 min
6	Ac-E_2(FKFE)$_2$-NH_2	11.65	Isocratic 5% **B** 5 min, 5-95% **B** over 10 min, 95% **B** 5 min
7	Ac-E_4(FKFE)$_2$-NH_2	11.36	Isocratic 5% **B** 5 min, 5-95% **B** over 10 min, 95% **B** 5 min
8	Ac-E_2(ChaKChaE)$_2$-NH_2	12.351	Isocratic 5% **B** 5 min, 5-95% **B** over 10 min, 95% **B** 5 min
9	Ac-E_4(ChaKChaE)$_2$-NH_2	12.114	Isocratic 5% **B** 5 min, 5-95% **B** over 10 min, 95% **B** 5 min

Figure S12. MALDI mass spectrum of Ac-$K_2(AKAE)_2$-NH_2.

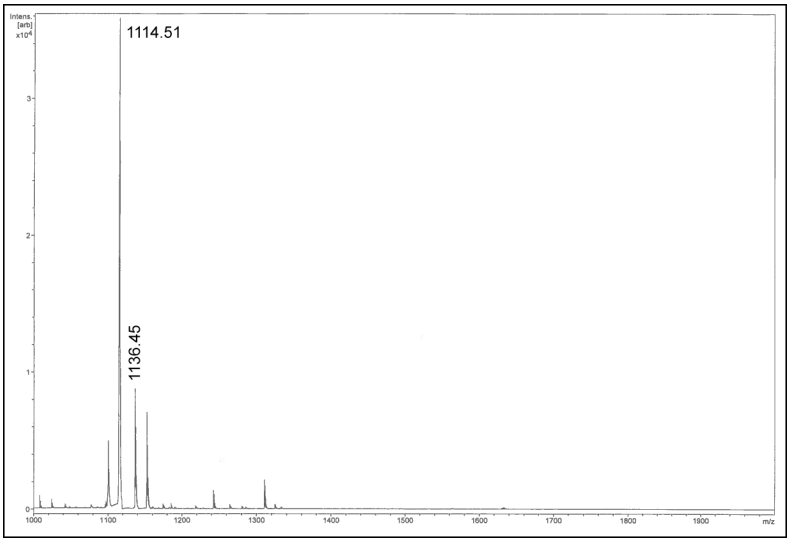

Figure S13. MALDI mass spectrum of Ac-$K_2(FKFE)_2$-NH_2.

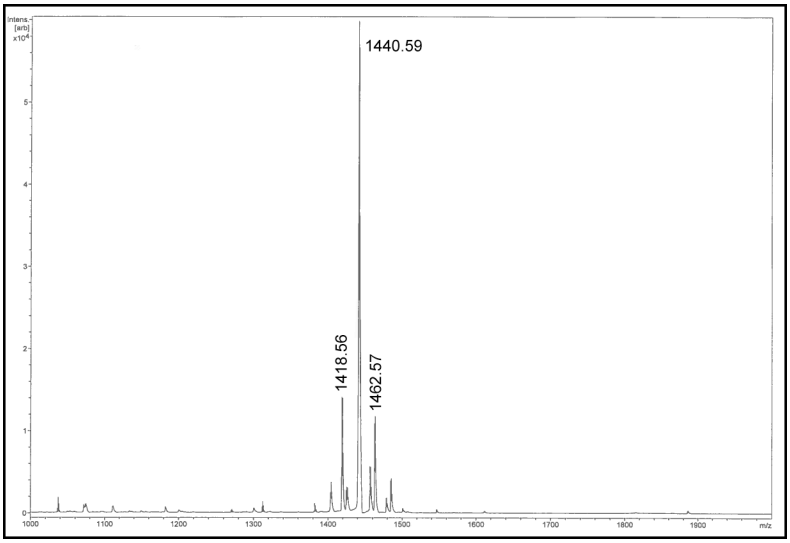

Figure S14. MALDI mass spectrum of Ac-$K_4(FKFE)_2$-NH_2.

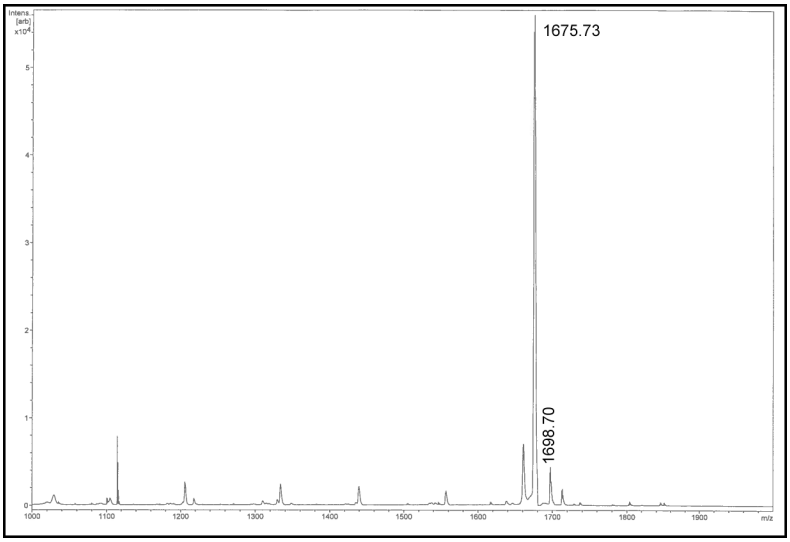

Figure S15. MALDI mass spectrum of Ac-$K_2(ChaKChaE)_2$-NH_2.

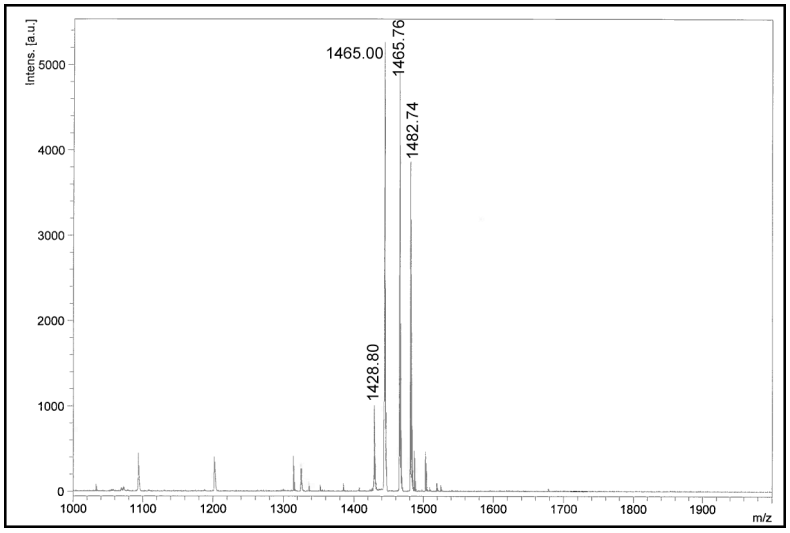

Figure S16. MALDI mass spectrum of Ac-K_4(ChaKChaE)$_2$-NH_2.

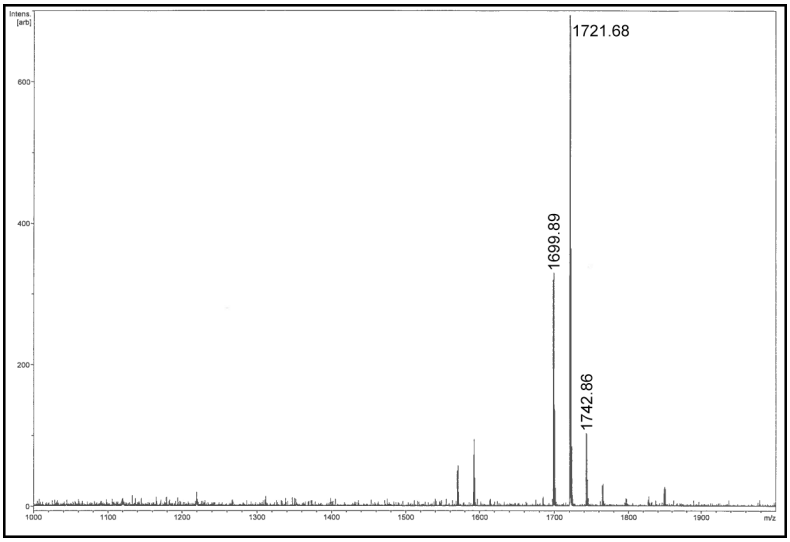

Figure S17. MALDI mass spectrum of Ac-E_2(FKFE)$_2$-NH_2.

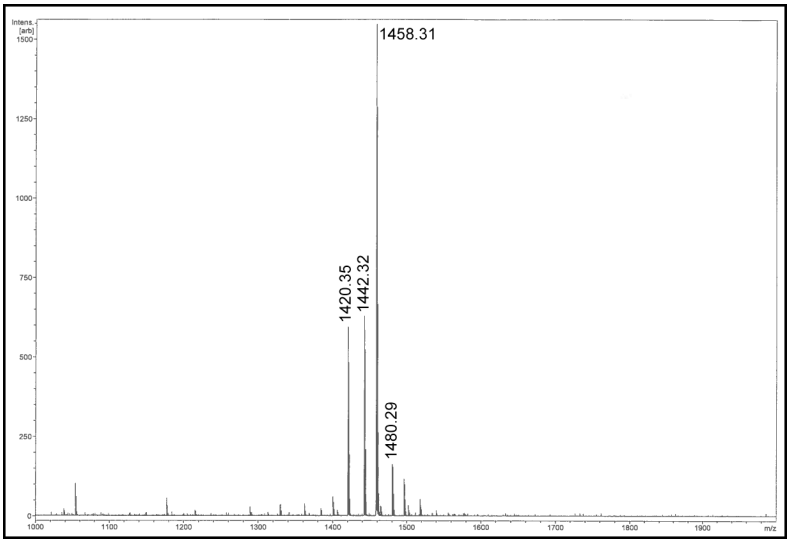

Figure S18. MALDI mass spectrum of Ac-$E_4(FKFE)_2$-NH_2.

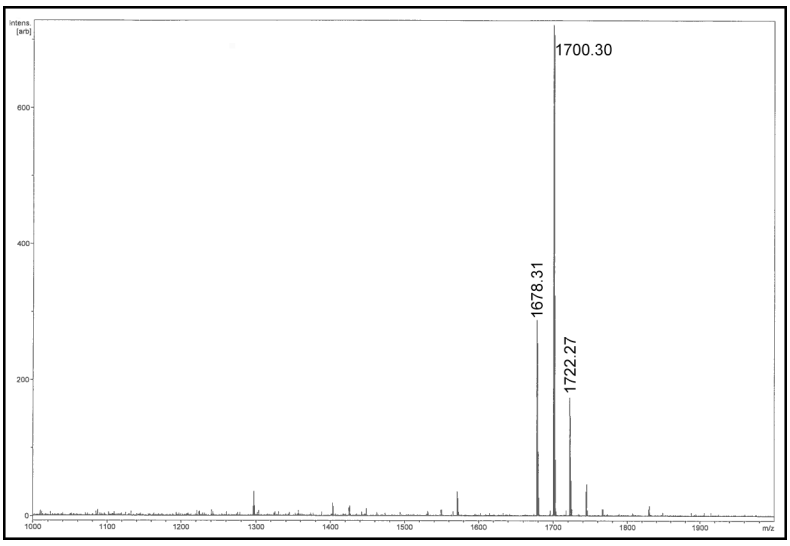

Figure S19. MALDI mass spectrum of Ac-$E_2(ChaKChaE)_2$-NH_2.

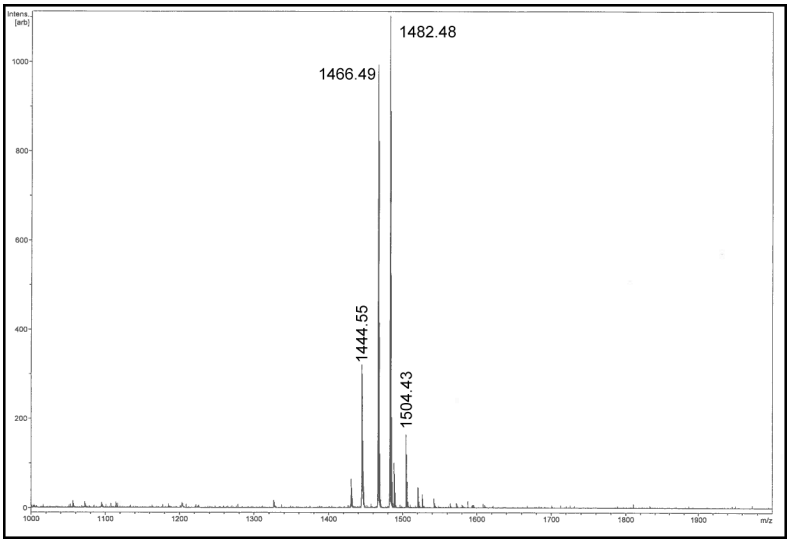

Figure S20. MALDI mass spectrum of Ac-E_4(ChaKChaE)$_2$-NH_2.

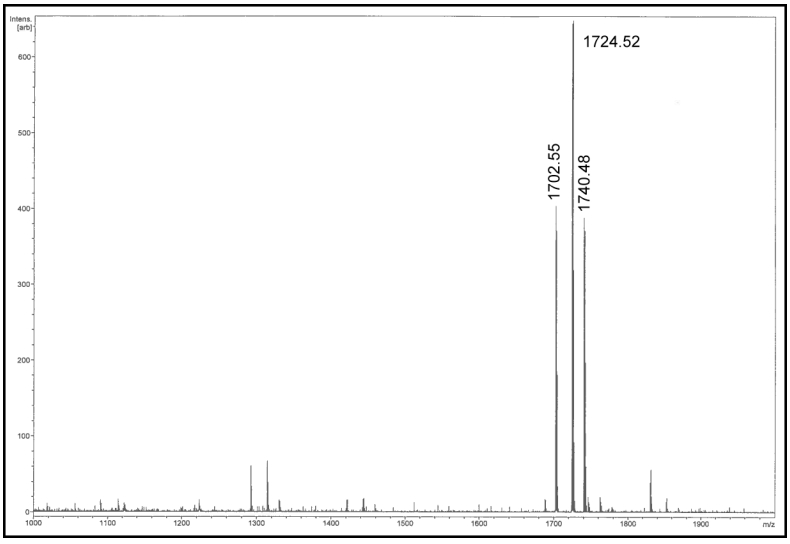

Figure S21. Visible appearance of peptide supramolecular assemblies. Glass vials containing supramolecular assemblies formed by $K_n(XKXE)_2$ and $E_4(ChaKChaE)_2$ test peptides and SEVI fibrils (assemblies of the PAP[248-286] peptide) are shown. All provide visual evidence of solubility except for SEVI fibrils (assemblies of the PAP[248-286] peptide), which are turbid. Peptides are as follows:
(A) SEVI fibrils in PBS: [peptide] = 1.33 mM, [NaCl] = 150 mM
(B) $K_2(FKFE)_2$ in deionized water: [peptide] = 1 mM, [NaCl] = 300 mM;
(C) $K_4(FKFE)_2$ in deionized water: [peptide] = 1 mM, [NaCl] = 300 mM;
(D) $K_2(ChaKChaE)_2$ in deionized water: [peptide] = 1 mM, [NaCl] = 300 mM;
(E) $K_4(ChaKChaE)_2$ in deionized water: [peptide] = 1 mM, [NaCl] = 300 mM;
(F) $E_4(ChaKChaE)_2$ in deionized water: [peptide] = 938 μM, [NaCl] = 300 mM, pH 7.

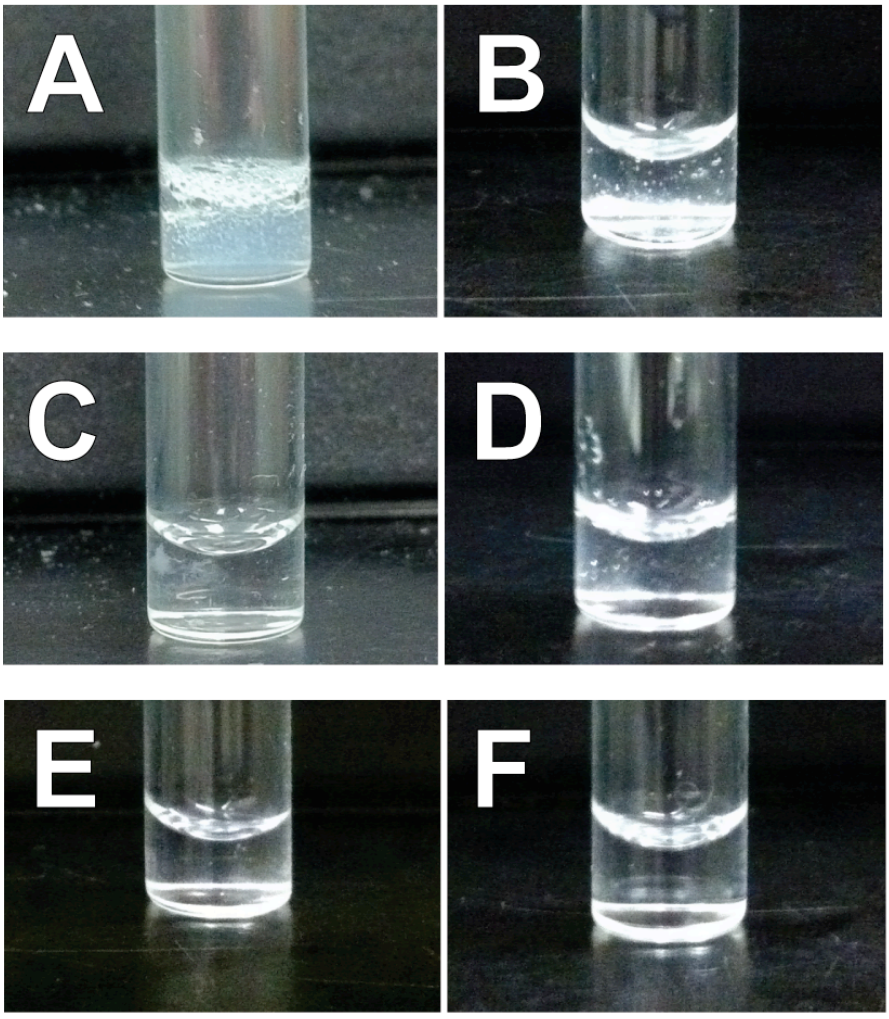

Figure S22. TEM images of peptide supramolecular assemblies, before and after removal of insoluble material by centrifugal sedimentation. TEM images are shown of supramolecular assemblies formed by $K_n(XKXE)_2$ and $E_4(ChaKChaE)_2$ test peptides and SEVI fibrils (assemblies of the PAP[248-286] peptide), either before or after high-speed centrifugation to remove sedimentable (insoluble) material. **(A-F):** Peptide stock peptide solutions were agitated and then imaged by transmission electron microscopy. **(G-L):** Peptide stock solutions were centrifuged at 14000 rpm at 4°C for 30 min. A portion of the supernatant material was then imaged by TEM. All the images show the presence of fibrils, regardless of centrifugal sedimentation of insoluble material, except for SEVI (panel **G**). Images are as follows:

Images of agitated (resuspended) peptides/aggregates:
(A) SEVI fibrils in PBS: [peptide] = 1.33 mM, [NaCl] = 150 mM
(B) $K_2(FKFE)_2$ in deionized water: [peptide] = 1 mM, [NaCl] = 300 mM;
(C) $K_4(FKFE)_2$ in deionized water: [peptide] = 1 mM, [NaCl] = 300 mM;
(D) $K_2(ChaKChaE)_2$ in deionized water: [peptide] = 1 mM, [NaCl] = 300 mM;
(E) $K_4(ChaKChaE)_2$ in deionized water: [peptide] = 1 mM, [NaCl] = 300 mM;
(F) $E_4(ChaKChaE)_2$ in deionized water: [peptide] = 938 μM, [NaCl] = 300 mM, pH 7.

Images of peptides/aggregates following centrifugal sedimentation of insoluble material:
(G) SEVI fibrils in PBS: [peptide] = 1.33 mM, [NaCl] = 150 mM
(H) $K_2(FKFE)_2$ in deionized water: [peptide] = 1 mM, [NaCl] = 300 mM;
(I) $K_4(FKFE)_2$ in deionized water: [peptide] = 1 mM, [NaCl] = 300 mM;
(J) $K_2(ChaKChaE)_2$ in deionized water: [peptide] = 1 mM, [NaCl] = 300 mM;
(K) $K_4(ChaKChaE)_2$ in deionized water: [peptide] = 1 mM, [NaCl] = 300 mM;
(L) $E_4(ChaKChaE)_2$ in deionized water: [peptide] = 938 μM, [NaCl] = 300 mM, pH 7.

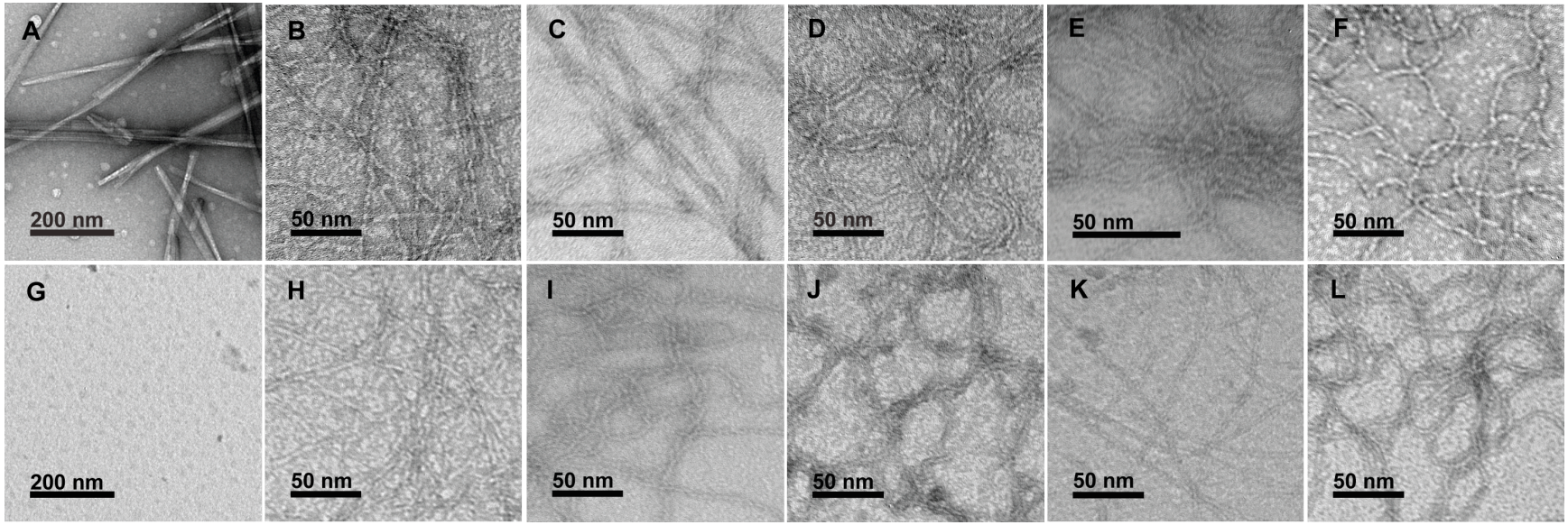
A
200 nm
B
50 nm
C
50 nm
D
50 nm
E
50 nm
F
50 nm
G
200 nm
H
50 nm
I
50 nm
J
50 nm
K
50 nm
L
50 nm

Figure S23. Cationic peptide supramolecular assemblies efficiently enhance low dose HIV-1 infection. CEMx M7 cells were infected with HIV-1 at a concentration 10-fold lower than that used in Figure 5 (i.e., at a concentration corresponding to 2.1 ng/mL of HIV-1 p24 antigen), in the presence of increasing concentrations of self-assembled peptides with (i) net positive charges (shown in red): SEVI, $K_4(FKFE)_2$, $K_2(FKFE)_2$, $K_4(ChaKChaE)_2$, $K_2(ChaKChaE)_2$, (ii) net negative charges (shown in blue): $E_4(FKFE)_2$, $E_2(ChaKChaE)_2$, and (iii) unassembled positively charged peptide (shown in orange): $K_2(AKAE)_2$. At 48 hours post infection cells were harvested and luciferase measured as a read out of HIV-1 infection. Results represent mean values from three experimental replicates; error bars denote the standard deviation of these values. *Notes: (1) all peptide concentrations refer to final concentrations in cell culture (and not to concentrations during virion pre-incubation, which were higher); (2) we have plotted the data on a semi-log scale, to facilitate comparison of values obtained at low concentrations. Since the log of zero is not defined, we were obliged to use a discontinous x-axis to do this. The far left portion of the x-axis is thus plotted with a linear (ordinary) axis, in order to accommodate the value x = zero.*

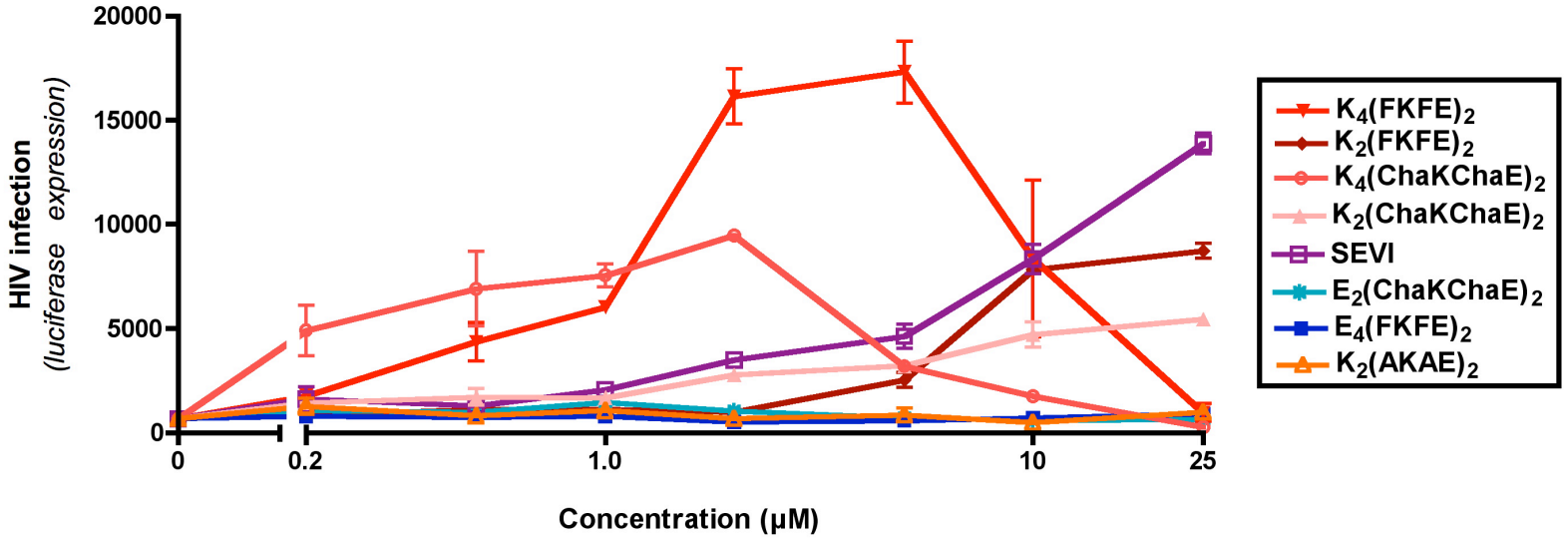

Figure S24. Cationic and anionic supramolecular assemblies are not cytotoxic *in vitro.* CEMx M7 cells were cultured for 24 hours **(A)** or 72 hours **(B)** in the continuous presence of increasing concentrations of fibrils (1, 10, 25 μM) in RPMI-1640 growth media containing 10% Alamar Blue®. After 24 hours **(A)** or 72 hours **(B)** metabolic activity was measured spectrophotometrically. The fluorescence values for untreated cells were assigned as 100% viability, and values for treated cells were then normalized to this. Results represent mean values from three experimental replicates; error bars denote the standard deviation of these values.

A

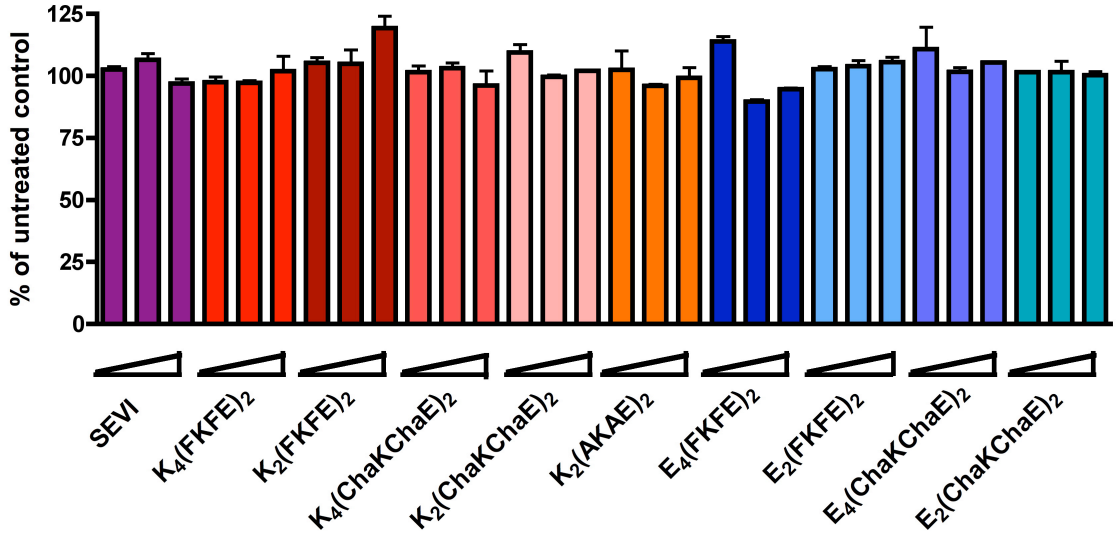

B